AVERAGE HARD X-RAY EMISSION FROM NS LMXBS: OBSERVATIONAL EVIDENCE OF DIFFERENT SPECTRAL STATES IN NS LMXBS

R. Farinelli[1], A. Paizis[2], L. Titarchuk[1,3,4], T.J.-L. Courvoisier[5,6], A. Bazzano[7], V. Beckmann[3,8], F. Frontera[1], P. Goldoni[9,10], E. Kuulkers[11], S. Mereghetti[2], J. Rodriguez[10], O. Vilhu[12]

[1]*Dipartimento di Fisica, Università di Ferrara, Via Saragat 1, I–44100 Ferrara, Italy, E-mail:farinelli@fe.infn.it*
[2]*INAF-IASF, Sezione di Milano, Via Bassini 15, I–20133 Milano, Italy, E-mail:ada@iasf-milano.inaf.it*
[3]*NASA Goddard Space Flight Center, Exploration of the Universe Division, Greenbelt, MD 20771, USA*
[4]*George Mason University/Center for Earth Observing and Space Research, Fairfax, VA 22030 and US Naval Research Laboratory, Code 7655, Washington, DC 20375-5352, E-mail:titarchuk@fe.infn.it*
[5]*INTEGRAL Science Data Centre, Chemin d'Ecogia 16, 1290 Versoix, Switzerland, E-mail:Thierry.Courvoisier@obs.unige.ch*
[6]*Observatoire de Genève, 51 chemin des Mailletes, CH–1290 Sauverny, Switzerland*
[7]*INAF-IASF, Sezione di Roma, Via del Fosso del Cavaliere 100, I-00133, Roma, Italy, E-mail:angela@rm.iasf.cnr.it*
[8]*Joint Center for Astrophysics, Department of Physics, University of Maryland, Baltimore County, MD 21250, USA, E-mail:beckmann@milkyway.gsfc.nasa.gov*
[9]*APC/UMR 7164, 11 Place M. Berthelot,75231 Paris, France, E-mail:paolo@discovery.saclay.cea.fr*
[10]*CEA, Centre de Saclay, DSM/DAPNIA/SAp, 91191 Gif-sur-Yvette Cedex France, E-mail:jerome.rodriguez@obs.unige.ch*
[11]*ISOC, ESA/ESAC, Urb. Villafranca del Castillo, PO Box 50727, 28080, Madrid, Spain, E-mail:ekuulker@rssd.esa.int*
[12]*Observatory, P.O.Box 14, Tähtitorninmäki, Fi–00014 University of Helsinki, Finland, E-mail:Osmi.Vilhu@Helsinki.Fi*

ABSTRACT

We studied and compared the long term average hard X-ray ($>$20 keV) spectra of a sample of twelve bright low-mass X-ray binaries hosting a neutron star (NS). Our sample comprises the six well studied Galactic Z sources and six Atoll sources, four of which are bright ("GX") bulge sources while two are weaker ones in the 2–10 keV range (H 1705–440 and H 1608–522). For all the sources of our sample, we analysed available public data and extracted average spectra from the IBIS/ISGRI detector on board *INTEGRAL*. The two low-dim Atoll spectra are dominated by photons upscattered presumably due to dynamical and thermal Comptonization in an optically thin, hot plasma. For the first time, we extend the detection of H 1705–440 up to 150 keV. The Z and bright "GX" Atoll source spectra are very similar and are dominated by Comptonized blackbody radiation of seed photons presumably coming from the accretion disc and NS surface. The seed photons radiation is Comptonized in the optically thick cloud with plasma temperature in the range of 2.5–3 keV. Six sources show a hard tail in their *average* spectrum: Cyg X-2 (Z), GX 340+0 (Z), GX 17+2 (Z), GX 5–1 (Z), Sco X–1 (Z) and GX 13+1 (Atoll). This is the first detection of a hard tail in the X-ray spectrum of the peculiar GX 13+1 that we discover to behave like a Z source not only in its variability and radio properties, but also from the spectral point of view. Using radio data from the literature we find, in all Z sources and bright "GX" Atolls, a *systematic* positive correlation between the X-ray hard tail (40–100 keV) and the radio luminosity. This suggests that hard tails and energetic electrons causing the radio emission may have the same origin, most likely the Compton cloud located inside the NS magnetosphere.

Key words: X-rays: binaries – binaries: close – stars: neutron.

1. INTRODUCTION

Low-Mass X-ray Binaries (LMXBs) are systems where a compact object, either a neutron star (NS) or a black hole candidate (BHC), accretes matter via Roche lobe overflow from a companion with a mass $M < M_{\odot}$. NS LMXBs can be broadly classified according to their timing and spectral properties ([8]). On the basis of this classification, NS LMXBs are divided in Z sources and Atoll sources from the shape of their track in the colour-colour diagram and on the different timing behaviour that correlates with the position on the tracks. The overall spectra of Z sources are very soft ([2] and references therein) and can be described by the sum of a cool ($\sim$1 keV) blackbody (BB) and a Comptonized emission from an electron plasma ("corona") of a few keV. Instead, Atoll sources perform quite dramatic spectral changes: when bright, they can have soft spectra (similar to Z sources) but they switch to low/hard spectra at low luminosities. So far, only Atoll sources (and more generally X-ray

bursters) have been observed with low/hard spectra (i.e. Comptonizing corona of few *tens* of keV). Z sources always have soft Comptonization spectra (energy of few keV) and can display an additional hard X-ray component dominating the spectrum above $\sim$30 keV. This component is on top of the soft spectrum and is highly variable with most of the emission remaining soft (see [1, 4] for a review on NS LMXB spectra).Hence, we would expect that the average high energy spectra of Atoll sources have a strong component above 30 keV and that in the soft Z sources this component is less prominent and smeared out in the time averaged spectrum. Z sources spend most of their time in the high/soft state, but they may show the transition to harder states at lower luminosity. The sensitivity of the past missions may have introduced an observational bias, similarly to the lack of a continuous coverage of the Galactic plane and Centre in the less explored hard X-ray range (above 20 keV). Moreover, the concentration of these sources towards the Galactic centre makes it difficult to observe them with non-imaging instruments. Consequently, data analysis and interpretation of such observations is extremely problematic. All these instrumental biases can be minimised with the use of the recently launched INTErnational Gamma-Ray Astrophysics Laboratory, *INTEGRAL* ([25]). The imager *INTEGRAL*/IBIS ([24]) has high sensitivity, about $\sim$10 times better than *GRANAT*/SIGMA, coupled to imaging capability with $12'$ angular resolution above 20 keV. In this paper we report the study of the average hard X-ray spectra of twelve NS LMXBs performed with the low energy (20–200 keV) IBIS detector, ISGRI ([9]), using a coherent and large sample of data, free from systematic effects which play a role when combining data from different missions. The sample of the LMXBs chosen is given in Table 1 and comprises six Galactic Z sources and six Atoll sources, four of which are bright ("GX") bulge sources while two are weaker ones in the 2-10 keV range. Our approach is two-fold: on one side, for comparison purposes, we study the average spectra in terms of phenomenological models as done in the literature, on the other, we study the sources in the frame of a physical model in the attempt to find a self-consistent scenario that describes all the spectral properties we observe. We discuss the similarities of such a scenario with the black hole LMXB case as well as the radio - X-ray correlation that is typical of LMXBs.

Table 1. LMXBs studied in this paper. D*: distance (in kpc) from references in [10] except for (*) from [3] and (**) from [6];* Rate*: average 22–40 keV counts/sec of the source as obtained from the mosaic image reported in Fig. 1 of [12]. Multiply by $\sim$10 to obtain a flux estimate in units of mCrab. F(1mCrab)*$_{22-40\,keV}$ *$\sim 6.8\times10^{-12}$* erg s^{-1} cm^{-2}; *SNR*: signal to noise ratio in the 22–40 keV band; *MaxEn*: maximum energy channel (keV) with a signal to noise ratio higher than three in the average spectrum; T_{exp}: effective exposure time in ksec.

Source	D (kpc)	Rate (cps)	SNR	MaxEn (keV)	T_{exp} (ksec)
Z sources					
Sco X–1	2.8	58.3	1757	150	266
GX 340+0	11	2.4	124	46	433
GX 349+2	5	3.4	189	39	265
GX 5–1	9.2	3.8	330	80	1091
GX 17+2	14	4.4	203	80	248
Cyg X–2	13.3	2.2	57	55	149
Atoll sources					
H 1608–522	4**	0.8	36	150	299
H 1705–440	11**	3	144	150	307
GX 9+9	5*	0.97	55	35	139
GX 3+1	5.6*	0.96	86	43	2027
GX 9+1	7*	1.2	91	37	491
GX 13+1	7	0.96	57	80	290

2. OBSERVATIONS AND DATA ANALYSIS

We have analysed *INTEGRAL* data publicly available in which the sources in Table 1 were in the Fully Coded Field of View (FCFOV) of IBIS. The additional criterion of a minimum of good time of 1000 sec for IBIS/ISGRI led to a total of 2263 pointings each with variable exposure time (from about 1800 sec up to about 3600 sec) spanning from January 2003 to May 2004. Version 5.1 of the Off-line Scientific Analysis (OSA) software has been used to analyse the data. The description of the algorithms used in the IBIS/ISGRI scientific analysis can be found in [7]. For each pointing we extracted images in the 22–40 and 40–80 keV energy bands. The images were used to build light curves as well as a final mosaic. The mosaic images revealed the sources that were active in the field of view at the time of the observations. The list of all the detected sources (one per source of interest) was then used in the spectral step, where spectra for all the active sources in the field of view were simultaneously extracted with the standard spectral extraction method. The single pointing spectra were then averaged into one final spectrum per source. These final average spectra have been used in our spectral study adding 1% systematic error (with the exception of the bright Sco X–1 for which we added 1.5% systematic error). In the fit, only data points with more than 3σ in the 22–200 keV range have been considered. To cross-check our results, we also used the alternative method of extracting spectra from the mosaics. To do so, we re-ran the imaging step in twelve different bins (instead of the 22–40 and 40–80 keV, previously mentioned) for all the pointings and then extracted a spectrum using the flux from each energy map. We verified that the two different methods give compatible results. In the this work we show only the results of the former method (the standard extraction) for which we have a finer binning.

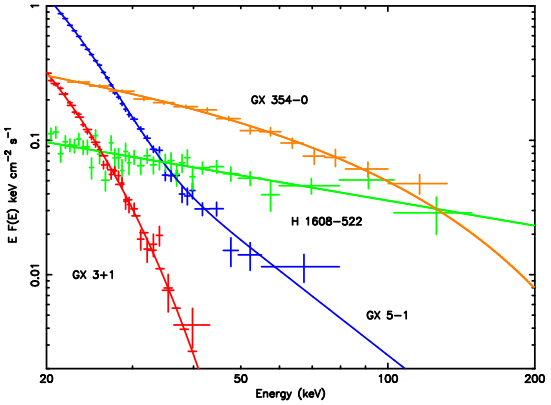

Figure 1. IBIS/ISGRI average spectra of GX 354-0 ("pure" low/hard state, see text), H 1608–522 (low/hard state), GX 5–1 (intermediate state) and GX 3+1 (very soft state) .

2.1. A phenomenological approach

As a first attempt we tried to fit all the spectra with the same simple model, in order to compare them directly. It soon turned out that this was not possible since the long term average spectra identified three main spectral states. Phenomenologically, we can classify them in terms of a widely used thermal Comptonization model , COMPTT by [18]. We found that the spectra of GX 349+2, GX 9+1, GX 9+9, and GX 3+1 are well described by a single COMPTT component while we need two components (thermal Comptonization plus powerlaw, COMPTT+PL) to describe the data for Sco X–1, GX 5–1, GX 340+0, GX 17+2, Cyg X–2 and GX 13+1. On the other hand the spectral shapes of H 1608–522 and H 1705–440 can be well fitted by a simple PL. By comparison with black hole LMXBs, hereafter we call the above spectral state fitted with a single COMPTT a *very soft* state for which the spectral shape is well described by the BB-like shape slightly modified by Comptonization. Using this analogy, we call our COMPTT+PL-state an *intermediate* state. In fact, the *intermediate* state in the BHCs is characterized by the BB-like component at low energies and the steep PL component at higher energies. In the low/hard state spectra of BHCs, the BB signature is smeared out but the PL is prominent. Keeping in mind this observational fact for the BHCs, we can call our ("PL") state a *low/hard* state. The three states are shown in Fig. 1, while in Figs. 2 and 3 we show the deconvolved EF(E) spectra and best fit models of all the sources. The best fit parameters of the model are reported in Table 2 of [12]. In the plot of Fig. 1 we have also included the spectrum of the Atoll source GX 354-0 ([5]) to point out that the *low/hard* state of our classification, associated to H 1608–522 in the plot, is not a "pure" low/hard state as in the case of GX 354-0 (thermal Comptonization with cut-off) but is a low/hard state where an additional physical mechanism producing a non-attenuated PL starts to be important.

2.2. Generic Comptonization Model

As we have mentioned above in our analysis of X-ray spectra from NS LMXBs, we found similarities with black hole LMXBs. The BHC and NS spectral shapes are generic: they consist of BB-like and PL components. Sometimes one needs an exponential rollover in order to terminate the PL component at high energies. The main difference is that NS spectra are usually softer for the same state. Another difference in these spectra is that in the NS case there are two BB components (not one as in BHC spectra) which can be related to the emission from the disc (BB colour temperature about 1 keV) and NS surface (BB colour temperature about 2.5 keV). References [20] and [21] introduced the Generic Comptonization model (BMC model in XSPEC). The BMC model reads as:

$$F(E) = \frac{C_N}{1+A}(BB + A \times BB * G) \qquad (1)$$

where $G(E, E_0)$ is the Green function obtained as a solution of radiative diffusion equation. BB stands for the injected BB-like spectrum, namely $BB \propto B_\nu(T_{col})$, $BB * G$ is a convolution of BB with the (Comptonization) Green function $G(E, E_0)$, C_N is the BB normalization coefficient (that depends on the compact object mass and distance to the source). The factor $1/(1+A)$ is the fraction of the seed photon radiation directly seen by the Earth observer, whereas the factor $A/(1+A)$ is the fraction of the seed photon radiation upscattered by the Compton cloud. For a more detailed description of the model we remind the reader to [20], [21] and [12]. The free parameters of the BMC model (apart from the normalization C_N) are the BB colour temperature, kT_{bb}, the spectral index α (photon index $\Gamma = \alpha + 1$) and $\log A$.

It is worth noting that the BMC model is a generic Comptonization model which can be applicable for any type of Comptonization. The only limitation to its applicability is that the upper limit of the photons energy should be less than the mean energy of the plasma. In this case the Comptonization Green function is a broken PL (see [14], [16] and [17]). The Green function shape does not depend on the nature of the central object (NS or BHC) and it is also independent of the type of Comptonization. The fact that the BMC model well fits the shape of the observed spectrum means that the data contain the information on the Comptonization power index α (no matter whether it has thermal and/or bulk origin), $\log A$, kT_s and the BB component normalization (see, e.g., [13]). It also means but that no other information in the data besides the above parameters which describe the efficiency Comptonization α (which is reciprocal of the Comptonization parameter Y), the seed photon energy kT_s and geometry of the illumination of the Compton cloud $\log A$. The results of the fits of our *INTEGRAL* spectra with the BMC model are reported in Table 2. It is worth noting that for GX 340+0, GX 349+2, GX 9+9 and GX 3+1 only kT_{bb} is well constrained. This is not surprising given that in their spectra only the thermal bump is unambiguously detected. The best-fit colour

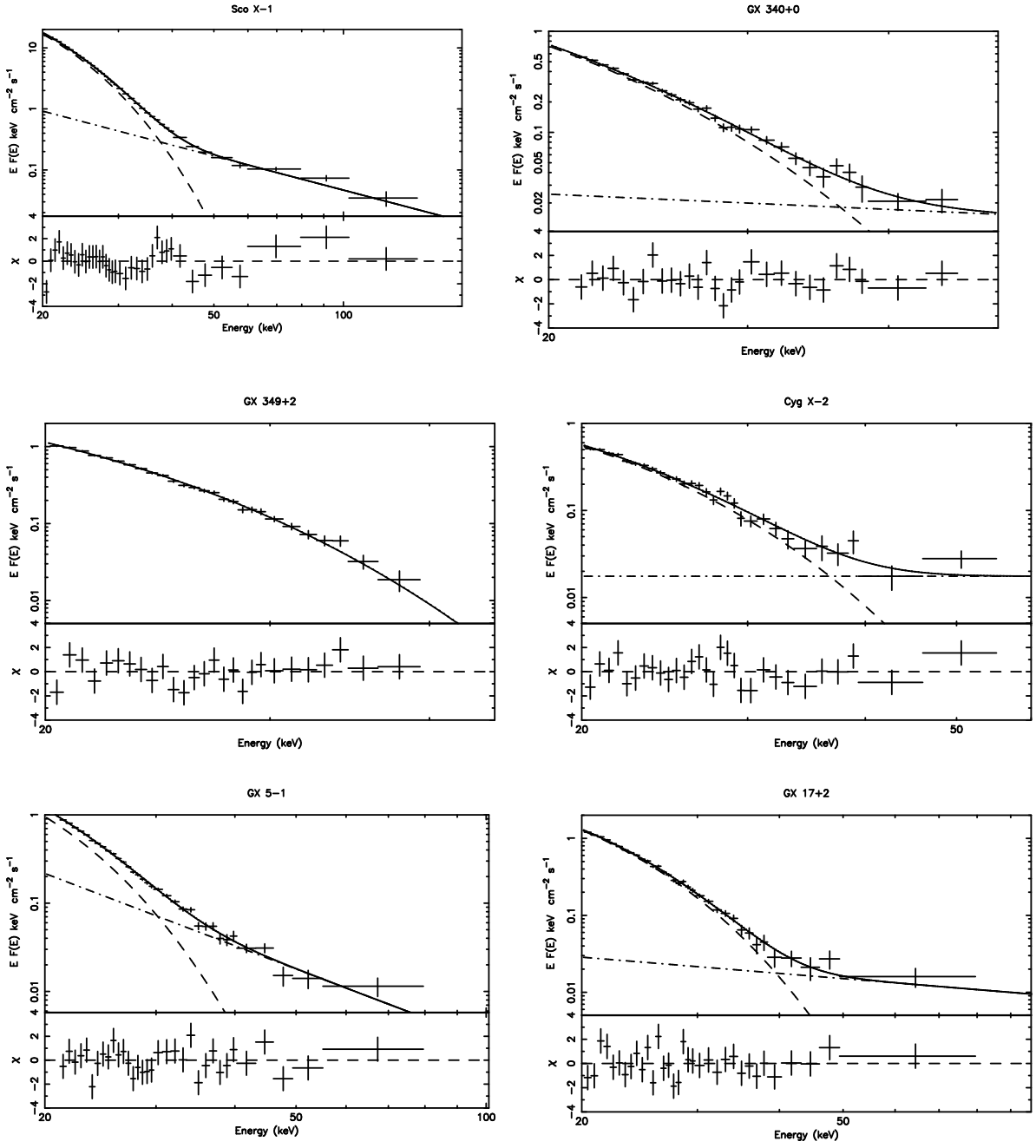

Figure 2. Z sources: average IBIS/ISGRI spectra and best fit model reported in Table 2 of [12].

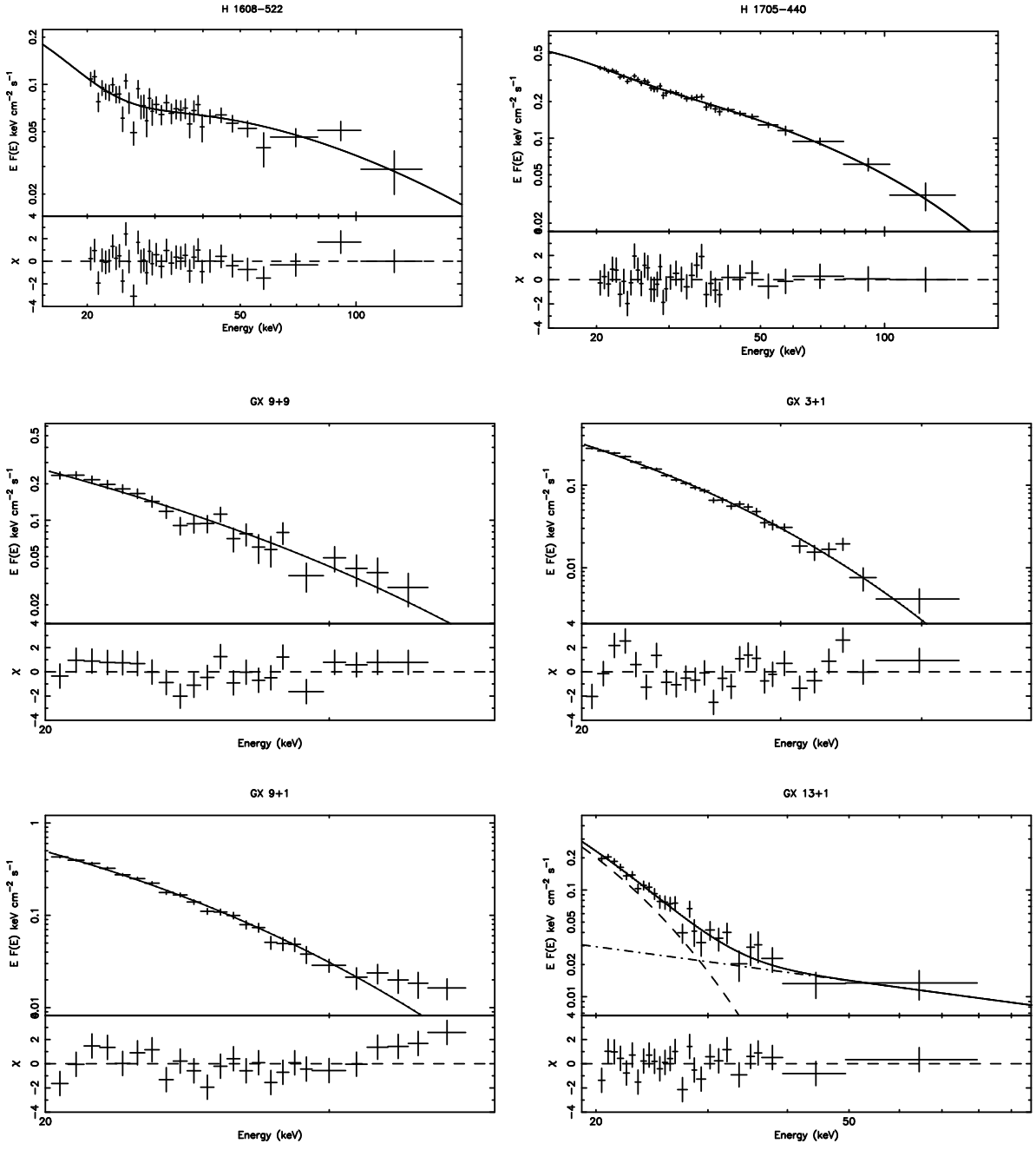

Figure 3. Atoll sources: average IBIS/ISGRI spectra and best fit model reported in Table 2 of [12] .

*Table 2. Best fit parameters for the bulk motion Comptonization model (*BMC*). No error means the parameter was fixed to the indicated value.* kT_{bb}*: BB colour temperature, in keV;* α*: energy spectral index (*Γ=α *+1);* $\log A$*: covering of the BB by the Compton cloud ;* $\mathrm{Flux}_{(20-40\,keV)}$*: flux obtained between 20–40 keV. For the sources detected up to 150 keV also the 40–150 keV flux is given.*

Source	kT_{bb} (keV)	α	$\log A$	χ^2/dof	$\mathrm{Flux}_{(20-40\,keV)}$ (erg s^{-1} cm^{-2})	$\mathrm{Flux}_{(40-150\,keV)}$ (erg s^{-1} cm^{-2})
Sco X–1	$2.56^{+0.01}_{-0.01}$	$3.27^{+0.06}_{-0.02}$	$-1.47^{+0.01}_{-0.01}$	68/35	5.8×10^{-9}	2.2×10^{-10}
GX 340+0	$2.43^{+0.18}_{-0.31}$	<6	$-1.12^{+0.81}_{-1.05}$	24/25	2.45×10^{-10}	
GX 349+2	$2.47^{+0.04}_{-0.12}$	<6	$-1.62^{+0.69}_{-1.03}$	20/23	3.5×10^{-10}	
GX 5–1	$2.35^{+0.07}_{-0.09}$	$3.84^{+0.72}_{-0.66}$	$-1.06^{+0.28}_{-0.26}$	34/30	3.75×10^{-10}	
GX 17+2	$2.68^{+0.06}_{-0.06}$	$2.0^{+1.46}_{-1.41}$	$-1.87^{+0.55}_{-0.42}$	32/30	4.5×10^{-10}	
Cyg X–2	$2.78^{+0.08}_{-0.07}$	<1.8	$-0.56^{+0.11}_{-0.14}$	26/26	2.1×10^{-10}	
H 1608–522	$1.49^{+1.39}_{-0.73}$	$1.50^{+0.14}_{-0.16}$	$-1.24^{+1.45}_{-2.5}$	39/34	8.5×10^{-11}	9.6×10^{-11}
H 1705–440	$0.84^{+0.14}_{-0.84}$	$2.15^{+0.05}_{-0.05}$	$-2.13^{+10.13}_{-3.85}$	36/35	2.9×10^{-10}	1.9×10^{-10}
GX 9+9	$2.53^{+0.18}_{-0.17}$	<6	$-0.70^{+0.34}_{-1.36}$	24/22	9.4×10^{-11}	
GX 3+1	$2.30^{+0.11}_{-0.14}$	<6	$-1.27^{+0.37}_{-1.32}$	42/23	9.3×10^{-11}	
GX 9+1	$2.20^{+0.05}_{-0.07}$	<3.2	$-1.09^{+0.16}_{-0.33}$	24/21	1.32×10^{-10}	
GX 13+1	$2.32^{+0.27}_{-0.36}$	$2.02^{+1.48}_{-1.33}$	$-1.34^{+0.58}_{-0.50}$	23/23	8.2×10^{-11}	

temperatures are about $2.5\,$keV using COMPTT or BB models. GX 17+2 and GX 13+1 have similar best-fit Γ-values, even if not well constrained whereas the slope of GX 5-1 is steeper but much better constrained than in GX 17+2 and GX 13+1. The upper value of Γ reported for Cyg X–2 (< 3) could be indicative of the presence of photon upscattering (Comptonization) of BB photons originated in the disc and NS surface. One can arrive to similar conclusions for GX 9+1 even if the effect seems to be less prominent there ($\Gamma < 4$). On the other side, for the two dim Atoll H 1608–522 and H 1705–440 we find that Γ is well constrained while there is no real information on kT_{bb}. This is not surprising given that in their spectra we do not see evidence of the thermal bump (described by the BB in the BMC model) and so it is impossible to infer either the BB colour-temperature or its relative contribution to the merging flux. It is worth noting that in Sco X-1, the whole set of the best-fit parameters is well constrained, given that both thermal bump and the hard tail are detected with high statistical significance.

3. DISCUSSION

We have analysed IBIS/ISGRI available public data on a sample of twelve persistent LMXBs containing a neutron star. As shown by their 22-40 keV and 40-80 keV light curves (see Figs. 2 and 3 in [12]), the sources have some degree of variability, which could somewhat complicate the analysis of their average spectra. This is true in particular for the two dim atolls H 1608–522 and H 1705–440, which show the highest degree of variability. Keeping this limitation in mind, it is worth emphasizing that the aim of the present work was not the detailed spectral study of a single source (which could not be possible with such approach), but rather the investigation of the high-energy (> 20 keV) *average* spectral properties of a sample of objects sharing some common properties (LMXBs hosting a weakly magnetized NS). The study of a population of sources, observed in different spectral states, is somewhat like taking pictures of a single one at different evolutionary stages. This is, for instance, the same approach used in the study of AGNs populations and in that of stars in globular clusters.

3.1. A scenario for spectral evolution in NS LMXBs

We observe three main spectral states: a very soft state with source spectra that can be well described by a single thermal Comptonization component, an intermediate state (thermal Comptonization plus PL) and a low/hard state (single PL). We have successfully studied these three spectral states in the frame of the Generic Comptonization Model (BMC, [20]). We present our scenario of the spectral evolution of NS LMXBs starting from the low/hard state. The *low/hard state* is characterized by a low mass accretion rate in the disc. In this case the gravitational energy release in the disc is much smaller than the one in the optically thin outer boundary of the corona (Compton cloud). The coronal outer boundary is presumably related to the adjustment shock ([19]). The corona completely covers the seed photon area (high $\log A$) and the emergent spectrum is a result of the upscattering (Comptonization) of the seed photons in the corona. One cannot see any trace of the seed photons in ISGRI (that give the BB bump). Open magnetic field lines are exposed to the observer but the outflow is weak because of the low mass accretion rate (there is not enough radiation in the disc to launch the wind) and the system is radio-

quiet. In the *intermediate state* the mass accretion rate increases with respect to the low/hard state. It leads to high efficiency of the Comptonization, particularly bulk inflow Comptonization that is seen as an extended hard tail in the spectrum. The thermal Comptonization becomes less efficient because the coronal plasma is cooled down by the seed photons coming from the disc and NS surface. The corona consists of a quasi-spherical component (related to the closed field lines and bulk motion inflow) and of a cylindrical component (related to the open field lines and outflow, [22]). The vertical size of the cylindrical configuration is suppressed as the mass accretion increases. We start to see the seed BB bumps (only the higher energy one in the IBIS/ISGRI range), because the corona is cooled down and becomes more compact. The *very soft* state is characterized by high mass accretion rate that is very close to the critical (Eddington) values. The emergent spectrum is a sum of two BB-like spectra, one is related to the Comptonization of the NS photons (visible in the IBIS/ISGRI range) and the other one is related the Comptonization of the disc photons. The seed photon and plasma temperatures differ by factor of a few. The electron plasma and the photons in the Compton cloud are very close to equilibrium. In this state the corona is quasi-spherical, there is no bulk motion and no radio emission. In fact, the radiation pressure caused by the strong emission from the NS surface stops the bulk inflow and the high accretion rate changes the configuration of the field lines and the radio emission is quenched. We also want to emphasize that the evolution scenario of LMXBs presented by us, in which the efficiency of bulk Comptonization (directly related to the accretion rate and to the consequent radiation pressure coming from the NS) plays a key role in determination of the spectral state for a given source is not just an *ad hoc* assumption about the presence of such a physical process, but in contrary it is based on theoretical expectations. Indeed, [23] calculate the radial velocity profile v_r in the transition layer between the geometrically thin accretion disk and the NS surface; starting from the consideration that the radial velocity equals the magneto-acoustic velocity v_{ma} at the outer (adjustment) radius of this transition layer (*postshock region*), R_{adj}, they find that v_r is very close to v_{ma} in the zone between the adjustment radius R_{adj} and some radius R_{ff} below which the accretion onto NS occurs in almost free-fall, radiation pressure-corrected, manner. The position of R_{adj} is not put by hand, but can be determined from the angular momentum transfer equation ([15]) and, for a given viscosity in the disk, it depends on the mass accretion rate only. Reference [11], using Monte Carlo simulations, showed that the importance of bulk motion Comptonization becomes negligible above $\sim$ 80 keV (this upper limit depending on the accretion rate), and thus could not explain the extended PLs observed in BHCs soft states (or those observed in NS LMXBs belonging to the Z class or the newly discovered one in GX 13+1). However, in their calculations there are some points which are not fully clarified: in particular, the optical depth along the beam path between A and B points is different for AB and BA segments, and the reason for this is not clear. Their calculations also show that bulk motion is much less important for spectral formation than thermal Comptonization even with free-fall velocities and any residual angular momentum will mean it accretes rather more slowly, so bulk motion effects will be smaller. We note however that it is not possible to say *a priory* that thermal Comptonization is anyway dominant over bulk dynamical one, given that the relative contribution among them strongly depends on the plasma temperature. In fact, [17] showed that if the plasma temperature of the converging flow is less than 10 keV, bulk Comptonization is the dominant process in the formation of the emergent spectrum, while for plasma temperature higher than 50 keV the resulting spectrum is formed mostly due to thermal Comptonization. This is in agreement with our results, where we show that the hard tails observed in Z sources (and GX 13+1), whose typical plasma temperatures are $\sim$ 3 keV (see, e.g., [4] for a review), are produced by bulk motion Comptonization, while those observed in H 1608–522 and H 1705–440 are the result of thermal Comptonization processes ($kT_{\rm e} \sim 120$ keV and $kT_{\rm e} \sim 50$ keV, respectively, when fitting their spectra with a thermal Comptonization model, see Table 2 in [12]).

A quantitative analysis of the sources X-ray and radio properties (see Table 4 in [12]) has revealed a clear connection of the emission in the two wavelength regimes. This correlation suggests that the hard tail formation area and the source of the energetic electrons, ultimately causing the radio emission, are closely connected. The most probable site of this configuration is the NS magnetosphere. It can be suggested that the open magnetic field lines of the NS magnetosphere are the base of the jet seen in the radio emission. An increasing accretion rate leads to a more efficient radio emission (low/hard state to intermediate state) up to a point where the extremely high accretion rate (very soft state) changes the configuration of the field lines and the radio emission is quenched.

REFERENCES

[1] Barret, D. 2001, Advances in Space Research, 28, 307

[2] Barret, D. & Olive, J.-F. 2002, ApJ, 576, 391

[3] Christian, D. J. & Swank, J. H. 1997, ApJs, 109, 177

[4] Di Salvo, T. & Stella, L. 2002, in Proc. of the XXXVIIth Rencontres de Moriond, *The Gamma-Ray Universe*, Ed. A. Goldwurm, Doris N. Neumann and Jean Tran Thanh Van, 67

[5] Falanga, M., Gotz, D., Goldoni, P., et al. 2006, A&A, in press [arXiv:astro-ph/0607330] 25

[6] Ford, E. C., van der Klis, M., Méndez, M., et al. 2000, ApJ, 537, 368

[7] Goldwurm, A., David, P., Foschini, L., et al. 2003, A&A, 411, L223

[8] Hasinger, G. & van der Klis, M. 1989, A&A, 225, 79

[9] Lebrun, F., Leray, J. P., Lavocat, P., et al. 2003, A&A, 411, L141

[10] Migliari, S. & Fender, R. P. 2006, MNRAS, 366, 79

[11] Niedzwiecki, A. & Zdziarski, A. A. 2006, MNRAS, 365, 606

[12] Paizis, A., Farinelli, R., Titarchuk, L., et al. 2006, A&A, 459, 187

[13] Shaposhnikov, N. & Titarchuk, L. 2006, ApJ, 643, 1098

[14] Sunyaev, R. & Titarchuk, L. 1980, A&A, 86, 121

[15] Titarchuk, L., Lapidus, I., & Muslimov, A. 1998, ApJ, 499, 315

[16] Titarchuk, L., & Zannias, T. 1998, ApJ, 493, 863

[17] Laurent, P. & Titarchuk, L. 1999, ApJ, 511, 289

[18] Titarchuk, L. 1994, ApJ, 434, 570

[19] Titarchuk, L. & Fiorito, R. 2004, ApJ, 612, 988

[20] Titarchuk, L., Mastichiadis, A., & Kylafis, N. D. 1996, A&As, 120, 171

[21] Titarchuk, L., Mastichiadis, A., & Kylafis, N. D. 1997, ApJ, 487, 834

[22] Titarchuk, L. & Shaposhnikov, N. 2005, ApJ, 626, 298

[23] Titarchuk, L. & Farinelli, R., 2007, in preparation

[24] Ubertini, P., Lebrun, F., Di Cocco, G., et al. 2003, A&A, 411, L131

[25] Winkler, C., Courvoisier, T. J.-L., Di Cocco, G., et al. 2003, A&A, 411, L1